



HAL
open science

Electromagnetic Heat-induced in Meso-structures: Computation of Temperature in Metallic Dimers

Dominique Barchiesi, Thomas Grosgees, Eric J. Kremer, Marc Lamy de La
Chapelle

► **To cite this version:**

Dominique Barchiesi, Thomas Grosgees, Eric J. Kremer, Marc Lamy de La Chapelle. Electromagnetic Heat-induced in Meso-structures: Computation of Temperature in Metallic Dimers. Progress in Electromagnetics Research Symposium, Mar 2011, Marrakech, Morocco. pp.406-410. hal-00631578

HAL Id: hal-00631578

<https://hal.science/hal-00631578v1>

Submitted on 12 Oct 2011

HAL is a multi-disciplinary open access archive for the deposit and dissemination of scientific research documents, whether they are published or not. The documents may come from teaching and research institutions in France or abroad, or from public or private research centers.

L'archive ouverte pluridisciplinaire **HAL**, est destinée au dépôt et à la diffusion de documents scientifiques de niveau recherche, publiés ou non, émanant des établissements d'enseignement et de recherche français ou étrangers, des laboratoires publics ou privés.

Electromagnetic Heat-induced in Meso-structures: Computation of Temperature in Metallic Dimers

D. Barchiesi¹, T. Grosjes¹, E. Kremer², and M. Lamy de la Chapelle³

¹Project Group for Automatic Mesh Generation and Advanced Methods

Gamma3 Project (UTT-INRIA), University of Technology of Troyes, France

²XLIM, Department of OSA, CNRS-UMR 6172, University of Limoges, France

³CSPBAT CNRS-FRE3043, UFR SMBH, University of Paris 13, France

Abstract— The illumination of a dimer metallic nanostructure is known to produce an intense source of light, with nanometric size. This confinement of light in the gap between the two material structures can induce an increase of the absorption of the electromagnetic energy in the nanoantenna itself, and therefore its warm-up. The multiphysics problem associated to this photo-thermal effect is modeled through a Finite Element Method (FEM). This contribution consists in computing both the electromagnetic field and the temperature, and discussing the influence of the gap, in the case of a bow-tie nanoantenna. The applications could be the development of nanodevices with thermal properties.

1. INTRODUCTION

The concept of micro-thermic was recently introduced in nanotechnology [1, 2]. The topics of interest were essentially the thermal radiations of Atomic Force Microscope (AFM) and the thermal gradient distribution [3, 4]. Nevertheless, only a few experimental data on the thermal properties of nano-materials are available [5, 6] but a large new field of investigation is open, experimentally and theoretically, on the thermal effects at the micro and nanoscale [7, 8]. The fluorescence lifetime of molecules in the vicinity of metallic nanostructures is known to depend on materials and separation [9, 10] but also on temperature. Therefore, a temperature mapping near nanostructures has been recently proposed, by measuring fluorescence anisotropy [6]. Despite this lack, it is straightforward that laser induced effects can lead to non negligible thermal effects on near-field optics probes. Therefore, it becomes necessary to develop theoretical and numerical models in photo-thermics [11, 12] in order to predict the elevation of temperatures in such structures.

Among the family of nanosensors and nanodevices, the nanoantennas that are of great interest in various engineering domains (optics, photonics, biology...), the bow-tie nanoantennas support multiple resonances and have promising spectral properties [13, 14]. In such dimer nanoantennas, a strong field enhancement appears in the gap, depending on material and geometry of the two top-to-tail gold triangles [13, 15] which can lead to act as thermal nanometric source [16].

In this paper, we investigate the influence of the gap which is a critical parameter of nanoantennas, on the photo-induced heating, through FEM solving of the electromagnetic and thermic partial differential equations, in a (2D) geometry. The paper is organized as follows. Section 2 is devoted to describe the method used to compute the coupled partial differential equations (PDE), including optical and thermal contributions. In Section 3, a discussion on the physical parameters, and numerical results are given. The application to bow-tie nanoantenna are presented and discussed, before concluding.

2. MODEL AND FEM FORMULATION

FEM has proved to be an efficient method for the computation of electromagnetic field around nanostructures [8]. The main advantages of the FEM are first its ability to treat any type of geometry and material inhomogeneity (with complex permittivity) [8], second the control of the accuracy of computation to evaluate accuracy of solutions, by using a non regular mesh of the domain of computation. The FEM is also known to be efficient in the resolution of multiphysics problems as well as non linear ones.

The PDE system is formed of the Helmholtz' for non-magnetic material with harmonic time dependence, and the Poisson's equations (the stationary heat equation, coupled by a source term

in the second one [12]:

$$\left[\nabla \cdot \left(\frac{1}{\epsilon_r(y, z)} \nabla \right) + \frac{\omega^2}{c^2} \right] H_x(y, z) = 0 \quad (1)$$

$$[\nabla \cdot (\lambda(y, z) \nabla)] T(y, z) + \frac{\omega \epsilon_0 \Im(\epsilon_r(y, z))}{2} |\mathbf{E}(y, z)(\epsilon_r)|^2 = 0, \quad (2)$$

where $\nabla = (\partial_x, \partial_y, \partial_z)$ is the differential vector operator, in cartesian coordinates, \cdot is the scalar product, c is the speed of light in vacuum, ω the angular frequency of the monochromatic wave, $\lambda(y, z)$, the thermal conductivity, $\epsilon_r(y, z)$ the relative permittivity of media, and ϵ_0 , the permittivity of vacuum. The shape of the gold bow-tie nanoantenna is defined in the (y, z) plane, as the electric field $\mathbf{E}(y, z)$ which is deduced from the magnetic field $H(y, z)$ along x direction, through the Maxwell-Ampere's equation.

The boundary conditions result from the integration of the PDE and therefore from the flux continuity [17]:

$$\mathbf{n}_{12} \cdot \left[\left(\frac{1}{\epsilon_2} \nabla H_2 \right) - \left(\frac{1}{\epsilon_1} \nabla H_1 \right) \right] = 0 \quad \text{and} \quad \mathbf{n}_{12} \cdot [(\lambda_2 \nabla T_2) - (\lambda_1 \nabla T_1)] = 0 \quad (3)$$

where \mathbf{n}_{12} is the normal to the boundary vector, ϵ_k , $k = 1, 2$, are the complex permittivity and λ_i , the thermal conductivity of the nanoantenna and surrounding medium respectively. The electromagnetic boundary condition (Eq. (3)) in 2D geometries, is formally equivalent to the continuity of the tangential component of the electric field. The boundary conditions on the fictitious external boundary of the domain of computation (vacuum), corresponding to the free propagation of the diffracted field $H_2 - H_i$ [17] and to the incoming illumination H_i , are defined by:

$$\mathbf{n}_{12} \cdot [(\nabla H_2)] = j [\mathbf{k} \cdot \mathbf{n}] \vec{H}_i + j \frac{\omega}{c} (H_2 - H_i) \quad \text{and} \quad \mathbf{n}_{12} \cdot [(\lambda_2 \nabla T_2)] = 0, \quad (4)$$

where H_i is the illuminating monochromatic, lying along x , magnetic field: $H_i = H_i^0 \exp(j\omega t - j\mathbf{k} \cdot \mathbf{r})$, with $\mathbf{k} = (0, \omega/c, 0)$, the wave vector, and j the square root of -1 . The solution of this FEM formulation, including a improved remeshing procedure, has been checked and compared with rigorous Mie theory [18–20]. To evaluate the temperature, the power P of the laser and the numerical aperture NA of the objective lens used to focus the beam of power on the nanoantenna must be used to calculate the amplitude of the incoming magnetic field: $H_i^0 = \omega \frac{NA}{1.22} \sqrt{\frac{2P\pi\epsilon_0}{c}}$.

3. PHYSICAL PARAMETERS AND NUMERICAL RESULTS

In the photo-thermal problem, two parameters are involved: the relative permittivity $\epsilon_r(y, z)$ and the thermal conductivity $\lambda(y, z)$. The relative permittivity appears in both Equations (1) and (2) and is consequently a critical parameter for the heating computation. Nevertheless, unlike models of phase change [8], we can suppose that there are no variations of material properties or of geometry of the nanoantenna. Actually, the temperature elevation is supposed to be small enough to be able to neglect dilations [6, 11]. The corresponding correction of the optical properties of such nanostructures has been rarely introduced, for the following reasons that are directly related to the typical size L of the nanostructures:

- No quantum effects are observed at this scale in metallic structures. As to it, the thermal De Broglie wavelength of a conduction electron in the gold nanostructure being Λ , the quantum effect can be neglected if the mean-free path of electrons is greater than $\Lambda = 4$ nm.
- the thermal dilation of nanostructures is neglected and therefore, neither variation of density nor change in optics properties has been took into account [21].
- Indeed, the size of each triangle of the bow-tie is almost one order of magnitude greater than the nanometric critical size for bulk permittivity validity of gold spherical nanoparticles [22]. If the size of the nanostructure is smaller than the bulk mean-free path of electron in gold ($l_e \approx 42$ nm), the effective mean-free path of electron is reduced typically to the size of the nanostructure [23]. Moreover, the mean-free path of photon in a gold sphere of radius 45 nm, for $\lambda_0 = 600$ nm, through Mie theory has been found to be smaller than the bulk value: 11 nm [24]. Nevertheless, the non negligible decrease of the imaginary part of the

permittivity of nanostructures has been observed for silver nanowires by fitting models with experiments [25]. In that paper, the imaginary part of the effective permittivity of silver has been shown to be the bulk one divided by three.

Therefore, even if in the investigated case of nanoantenna, the size L of the nanoantenna verifies $L > l_e > \Lambda$, a correction of the imaginary part of the permittivity is proposed to take into account the balance between diffusive and ballistic electrons in the nanostructures. The correction of the imaginary part of the permittivity $\Im(\epsilon_r)$, which is proportional to the electric conductivity of material, is deduced from the model described in [26]. The ratio of the imaginary part of the permittivity of the nanomaterial (ϵ_r) to the bulk one (ϵ_b) is known for nanowires [26]: $\Im(\epsilon_r) = C\Im(\epsilon_b) = [1 + \frac{3}{16}(1-p)l_e\frac{3L}{S}]^{-1}\Im(\epsilon_b)$, where p is the fraction of electrons scattered elastically at the surface of material, $l_e = 42$ nm the electron mean-free path in bulk gold, $3L$ the perimeter of the triangular cross-section and $S = L^2\sqrt{3}/4$ the cross-sectional area.

The evaluation of C for bow-tie shape remains open and therefore, we evaluate its variation for p in the interval $[0; 1]$, including the geometry of each nanostructure of the bow-tie antenna: $C \in [0.71; 1]$. Usually the parameter p is estimated to get the best fit with experimental data. In the following, $C = 0.83$ is used, corresponding to an equal contribution of diffuse and specular reflections of electron at surface, $p = 0.5$, and therefore, $\epsilon_r = -9.5 + j$ for gold at $\lambda_0 = 632.8$ nm (instead of $\epsilon_r = -9.5 + 1.22j$ for bulk material). This correction induces the decrease of the source term of the heat equation (Eq. (2)). The imaginary part of the permittivity of gold appears in Eqs. (1)–(2)) as a pure factor and therefore, the temperature variation in gold is proportional to it.

The choice of the edges $L = 2r\sqrt{\frac{\pi}{\sqrt{3}}} = 134$ nm of the equilateral triangular shapes of the bow-tie nanoantenna is governed to maintain the equivalent surface of matter equal to its of a cylindrical particle with radius $r = 50$ nm used in the above correction of constants [26]. This typical size is three times greater than the bulk mean-free path of electrons in gold ($l_e = 42$ nm). Therefore the condition $L > l_e > \Lambda$ is satisfied. The other numerical parameters of the photo-thermal problem are following in the SI system: $\omega = 2.9767 \cdot 10^{15}$ rad \cdot s $^{-1}$ (i.e., the wavelength in vacuum is $\lambda_0 = 632.8$ nm), $\epsilon_1 = (-9.5 + j)$, $\epsilon_2 = 1$, $P = 30$ mW, $NA = 0.6$, $\lambda_1 = 118$ W \cdot m $^{-1}$ \cdot K $^{-1}$, $\lambda_2 = 0.026$ W \cdot m $^{-1}$ \cdot K $^{-1}$. The radius of the domain of computation is 1 μ m. To avoid sharp tip effects in computations, we use quadratic polynomial of interpolation in the FEM formulation and spline rounding of the triangles vertices with 5 nm radius of curvature (Fig. 1(a)).

Figure 1(a) illustrate the refinement of the mesh where the electric field gradient is maximum. The length of the edges of the cells of the mesh is smaller than 0.2 nm, to describe accurately the skin effect in the vicinity of the interface between gold and air. With FEM, the accuracy is the maximum of the difference of the norms of unknowns ($|\mathbf{E}|$ and T respectively), between nodes and interpolation values along edges of each cell. This accuracy also called error, is lower than -30 dB (Fig. 1(b)) and therefore, the maximum of the variations of the computed solutions are lower than 10^{-3} between adjacent nodes. Moreover the insets in each figure show the acuteness of each unknown of the photothermal problem, related to the small mesh size shown in Fig. 1(a). Fig. 1(d) is the source term of the Poisson's equation, that can be compared to those in [12] for example. This source term exhibits a strong variation in gold. Its maximum is in the vicinity of the gap. Despite its shape, a first inspection of Fig. 1(e) shows an uniform heating of the whole structure as in Ref. [12]. The temperature elevation is more than 200 K, under the hypothesis that all the laser power (30 μ m) is concentrated in a zone of diameter 1.3 μ m, without loss of energy. An extrapolation of the curves in Fig. 3 of Ref. [11] with light flux of $2.3 \cdot 10^6$ W \cdot cm $^{-2}$, for nanospheres gives an elevation of temperature greater than 200 K, which is consistent with our results. Similarly, the PDE Equations (1) and (2), exhibit a difference of temperature, proportional to the incoming power. The obtained temperature elevation in gold is one order of magnitude greater than this in a single structure [6], but are consistent with the measurement of temperature in the gap of a rods dimer [12]. Actually, the temperature is directly related to the confinement of the intensity depends on the radius of curvature of the triangles vertices, on the

Instead of insulating boundaries, we also use effusive external boundaries, to enable a loss of thermal energy through the fictive external boundary but we do not observe induced variations of the elevation of temperature in gold. Thus, we are encouraged to conduct a study of the temperature variation depending on the gap. Fig. 1(f) shows the dependance of the intensity of the electric field, of the heat source and of the temperature variation, as functions of the gap. The homogenization of temperature in the whole nanostructure is responsible of the quasi-linear decrease of temperature

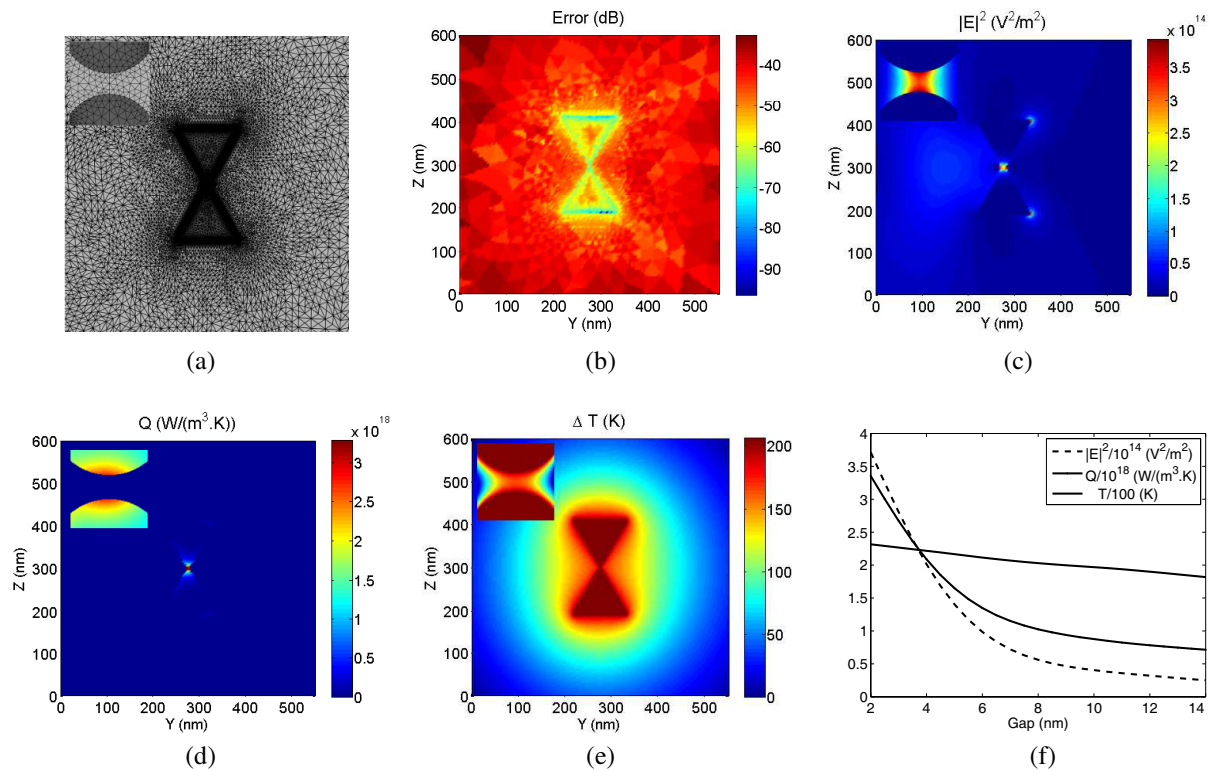


Figure 1: (a) Example of mesh. The distance between nodes can be much smaller than 0.1 nm to reach convergence [18]. The mesh is refined on the boundary of nanoantenna and in the gap, where the gradient of the electric field is maximum. (b) Global error evaluated on the mesh. (c) Intensity of the electric field for a gap of 2 nm. (d) Density of power absorbed in the gold nanostructure (source term of Eq. (2)). (e) Temperature elevation. (f) Variations as a function of the gap width for the maximum of electric field intensity, the maximum of the source term of the heat equation (in gold) and the elevation of temperature.

elevation, whereas the intensity and the source terms exhibits much stronger variations. gap and on the incoming power.

4. CONCLUSION

FEM has been applied to the computation of temperature elevation in bow-tie nanoantenna illuminated by a continuous laser. The photo-thermal heating strongly depends on the gap between the two dimers. From a theoretical discussion on the validity of the physical parameters used in the model as well as the careful bench of the numerical method, we deduce temperature elevations close to those reported in recent papers. Let us underline that the temperature variation depends on both imaginary part of the permittivity, and also on the thermal conductivity. This fact prohibits any attempt to recover equivalent thermal conductivity, directly from the temperature measurement of the nanostructures. This problem opens up an interesting thought about the resolution of the photothermal inverse problem. Regarding models, we plan to investigate two tracks of interest: the resolution of the problem with photothermal parameters obeying the laws of nonlinear behavior on the one hand, and secondly the transition in 3D.

ACKNOWLEDGMENT

This work was supported by the “Conseil Régional de Champagne Ardenne”, the “Conseil Général de l’Aube” and the *Nanoantenna* European Project (FP7 Health-F5-2009-241818).

REFERENCES

1. Ambrosio, A., M. Allegrini, G. Latini and F. Cacialli, “Thermal processes in metal-coated fiber probes for near-field experiments,” *Applied Physics Letters*, Vol. 86, 203109, 2005.
2. Kittel, A., W. Mller-Hirsch, J. Parisi, S.-A. Biehs, D. Reddig, and M. Holthaus, “Near-field heat transfer in a scanning thermal microscope,” *Physical Review Letters*, Vol. 95, 224301, 2005.

3. Erickson, E. S. and R. C. Dunna, "Sample heating in near-field scanning optical microscopy," *Applied Physics Letters*, Vol. 87, 201102, 2005.
4. De Wilde, Y., F. Formanek, R. Carminati, B. Gralak, P.-A. Lemoine, K. Joulain, J.-P. Mulet, Y. Chen, and J.-J. Greffet, "Thermal radiation scanning tunnelling microscopy," *Nature*, Vol. 444, 740–743, 2006.
5. Gucciardia, P. G., S. Paranè, A. Ambrosio, M. Allegrini, A. D. Downes, G. Latini, O. Fenwick, and F. Cacialli, "Observation of tip-to-sample heat transfer in near-field optical microscopy using metal-coated fiber probes," *Applied Physics Letters*, Vol. 86, 203109, 2005.
6. Baffou, C., M. P. Kreuzer, F. Kulzer, and R. Quidant, "Temperature mapping near plasmonic nanostructures using fluorescence polarization anisotropy," *Optics Express*, Vol. 17, 3291–3298, 2009.
7. La Rosa, A. H., B. I. Yakobson, and H. D. Hallena, "Origins and effects of thermal processes on near-field optical probes," *Applied Physics Letters*, Vol. 67, 2597–2599, 1995.
8. Grosgees, T., S. Petit, D. Barchiesi, and S. Hudlet, "Numerical modeling of the subwavelength phase-change recording using an apertureless scanning near-field optical microscope," *Optics Express*, Vol. 12, 5987–5995, 2004.
9. Pagnot, T., D. Barchiesi, and D. van Labeke, "Use of a scanning near-field optical microscope architecture to study fluorescence and energy transfer near a metal," *Optics Letters*, Vol. 22, 120–122, 1997.
10. Parent, G., D. van Labeke, and D. Barchiesi, "Fluorescence lifetime of a molecule near a corrugated interface: Application to near-field microscopy," *Journal of the Optical Society of America A*, Vol. 16, 896–908, 1999.
11. Govorov, A. O. and H. H. Richardson, "Generating heat with metal nanoparticles," *Nano Today*, Vol. 2, 30–38, 2007.
12. Baffou, G., C. Girard, and R. Quidant, "Mapping heat origin in plasmonic structures," *Physical Review Letters*, Vol. 104, 136805, 2010.
13. Fischer, H. and O. J. F. Martin, "Engineering the optical response of plasmonic nanoantennas," *Optics Express*, Vol. 16, 9144–9154, 2008.
14. Huang, J.-S., J. Kern, P. Geisler, P. Weinmann, M. Kamp, A. Forchel, P. Biagioni, and B. Hecht, "Mode imaging and selection in strongly coupled nanoantennas," *Nano Letters*, Vol. 10, 2105–2110, 2010.
15. Yang, L., C. Du, and X. Luo, "Numerical study of optical properties of single silver nanobow-tie with anisotropic topology," *Applied Physics B*, Vol. 92, 53–59, 2008.
16. Baffou, G., R. Quidant, and C. Girard, "Thermoplasmonics modeling: A Green's function approach," *Phys. Rev. B*, No. 82, 165424, 2010.
17. Jin, J., *The finite Element Method in Electromagnetics*, John Wiley and Sons, 1993.
18. Grosgees, T., A. Vial, and D. Barchiesi, "Models of near-field spectroscopic studies: Comparison between finite-element and finite-difference methods," *Optics Express*, Vol. 13, 8483–8497, 2005.
19. Borouchaki, H., T. Grosgees, and D. Barchiesi, "Improved 3D adaptive remeshing scheme applied in high electromagnetic field gradient computation," *Finite Element Analysis and Design*, Vol. 46, 84–95, 2010.
20. Grosgees, T., H. Borouchaki, and D. Barchiesi, "New adaptive mesh development for accurate near-field enhancement computation," *Journal of Microscopy*, Vol. 229, 293–301, 2008.
21. Rashidi-Huyeh, M. and B. Palpant, "Counterintuitive thermo-optical response of metal-dielectric nanocomposite materials as a result of local electromagnetic field enhancement," *Physical Review B*, Vol. 74, 075405, 2006.
22. Scaffardi, L. B. and J. O. Tocho, "Size dependence of refractive index of gold nanoparticles," *Nanotechnology*, Vol. 17, 1309–1315, 2006.
23. Moroz, A., "Electron mean free path in a spherical shell geometry," *Journal of Physical Chemistry C*, Vol. 112, 10641–10652, 2008.
24. Zhang, D. Z., G. Zheng, Z. Li, and J. Yang, "Mean free path of photon in gold suspension," *Optics Communications*, Vol. 105, 33–35, 1994.
25. Laroche, T., A. Vial, and M. Roussey, "Crystalline structure's influence on the near-field optical properties of single plasmonic nanowires," *Applied Physics Letters*, Vol. 91, 123101–123104, 2007.
26. Sondheimer, E. H., "The mean free path of electrons in metals," *Advances in Physics*, Vol. 50, 499–537, 2001.